Core Mutations That Promote the Calcium-Induced Allosteric Transition of Bovine Recoverin†

Anne N. Baldwin* and James B. Ames‡

Department of Neurobiology, Stanford University School of Medicine, Stanford, California 94305

Received April 23, 1998; Revised Manuscript Received July 17, 1998

ABSTRACT: Recoverin is a small calcium binding protein involved in regulation of the phototransduction cascade in retinal rod cells. It functions as a calcium sensor by undergoing a cooperative, ligand-dependent conformational change, resulting in the extrusion of the N-terminal myristoyl group from a hydrophobic pocket. To test the role of certain core residues in tuning this allosteric switch, we have made and characterized two mutants: W31K, which replaces Trp31 with Lys; and a double mutant, I52A/Y53A, in which Ile52 and Tyr53 are both replaced by Ala. These mutations decrease the hydrophobicity of the myristoyl binding pocket. They are thus expected to make sequestering of the myristoyl group less favorable and destabilize the Ca^{2+}-free state. As predicted, the myristoylated forms of the mutants exhibit increased affinity for Ca^{2+}, whether monitored by equilibrium binding of $^{45}Ca^{2+}$ (K_d = 17.2, 7.9, and 8.1 μM for wild type, W31K, and I52A/Y53A, respectively) or by the change in tryptophan fluorescence associated with the conformational change (K_d = 17.9, 3.6, and 4.4 μM for wild type, W31K, and I52A/Y53A, respectively). The mutants also exhibit decreased cooperativity of binding (Hill coefficient = 1.2 and 1.0 for W31K and I52A/Y53A vs 1.4 for wild type). Binding of the mutant proteins to rod outer segment membranes occurs at lower Ca^{2+} concentrations compared to wild-type protein ($K_{1/2}$ = 5.6, 2.2, and 1.0 μM for wild type, W31K, and I52A/Y53A, respectively). The unmyristoylated forms of the mutants exhibit biphasic Ca^{2+} binding curves, nearly identical to that observed for wild type. The binding data for the two mutants can be explained by a concerted allosteric model in which the mutations affect only the equilibrium constant L between the two allosteric forms, T (the Ca^{2+}-free form) and R (the Ca^{2+}-bound form), without affecting the intrinsic binding constants for the two Ca^{2+} sites. Two-dimensional NMR spectra of the Ca^{2+}-free forms of the mutants have been compared to the wild-type spectrum, whose peaks have been assigned to specific residues (*1*). Many resonances assigned to residues in the C-terminal domain (residues 100−202) in the wild-type spectrum are identical in the mutant spectra, suggesting that the backbone structure of the C-terminal domain is probably unchanged in both mutants. The N-terminal domain, in which both mutations are located, reveals in each case numerous changes of undetermined spatial extent.

Recoverin is a 200-residue calcium binding protein found in retinal rod cells, where it is believed to affect the phototransduction cascade by prolonging the lifetime of activated rhodopsin (*2*−*5*). Calcium sensors are important in the regulation of this pathway because activation of the phototransduction cascade results in the closure of cation channels, and a drop in intracellular Ca^{2+}. In the Ca^{2+}-bound state, recoverin is known to inhibit rhodopsin kinase in vitro (*6*−*9*), and thus can slow the turnoff of activated rhodopsin.

The reversible binding of two Ca^{2+} is mediated through EF-hand motifs first identified in parvalbumin (*10*) and later extensively characterized in troponin C (*11*) and calmodulin (*12*). A number of other homologous proteins are now known. Like the majority of these proteins, recoverin contains four EF-hand motifs arranged in pairs, each of which forms a helical bundle domain. In recoverin, the domains are tightly packed together. Only one binding site out of each pair is active, however, namely EF-2 and EF-3. Whereas in troponin C and calmodulin the binding of 2 mol of Ca^{2+} within each pair of EF hands is coupled, in recoverin, the linkage bridges the two domains. Ligand binding triggers a large conformational change of the N-terminal domain, and a rotation between the two domains. A myristoyl group attached to the N-terminal end is sequestered in the Ca^{2+}-free state (*13*) and becomes available for insertion into membranes only when the protein is in the Ca^{2+}-bound state (*14*). Thus, the conformational state of recoverin affects both its interaction with downstream effector proteins and its localization, and these two facets of its function are tightly coupled in what has been called the calcium−myristoyl switch (*14*). Understanding the detailed mechanism of this switch has been a major focus of this laboratory in the past few years.

When an X-ray structure of unmyristoylated recoverin with a single bound calcium ion revealed a major surface groove lined with hydrophobic residues (*15*), we designed several mutants to test whether these residues might interact with the myristoyl group and play a role in the conformational change. The residues we targeted included Trp31, Ile52, and Tyr53, whose orientations within the surface groove are

† Supported by NIH Grants EY02005-120 and GM24032-19.
* To whom correspondence should be addressed.
‡ Present address: CARB, 9600 Gudelsky Dr., Rockville, MD 20850.

10.1021/bi980928s CCC: $15.00
Published on Web 11/20/1998

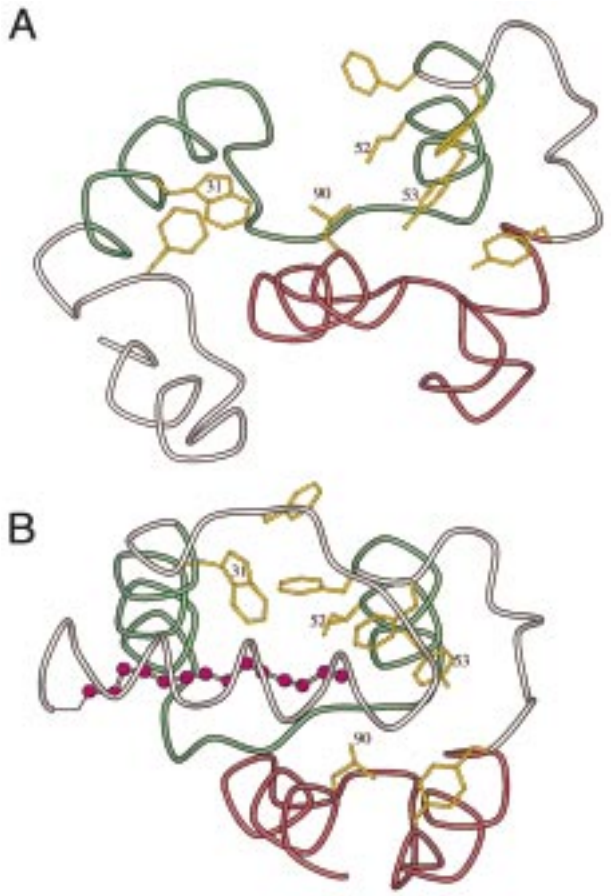

FIGURE 1: Orientation of Trp31, Ile52, and Tyr53 in the two conformations of wild-type recoverin. (A) Within the surface groove seen in the X-ray structure of unmyristoylated recoverin with one Ca^{2+} bound (*15*) and consistent with the NMR structure of myristoylated wild-type recoverin with two Ca^{2+} bound (*20*). (B) within the myistoyl binding pocket of Ca^{2+}-free recoverin based on the NMR structure of myristoylated protein (*13*). The myristoyl group is shown as a ball-and-stick representation (magenta). Hydrophobic side chain residues are shown in yellow.

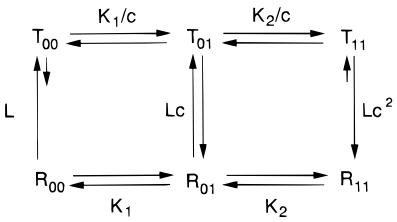

FIGURE 2: Concerted model for the binding of Ca^{2+} to recoverin.

shown in Figure 1A. All are conserved in the homologous proteins neurocalcin (*16*, *17*), hippocalcin (*18*), and frequenin (*19*). Subsequent NMR studies showed that these, as well as other aromatic residues, are indeed close to the myristoyl group in the Ca^{2+}-free state (*13*). In that state, however, they form part of the protein core, in which the myristoyl group is sequestered (Figure 1B). More recent NMR studies (20) have now demonstrated that the X-ray structure corresponds closely to the Ca^{2+}-bound conformation of myristoylated recoverin.

We had previously noted that recoverin behaves as an allosteric protein whose conformational change can be expressed by a two-state model (*21*) shown in Figure 2. This model resembles the original allosteric model of Monod, Wyman, and Changeux (*22*), without the requirement that the protein be oligomeric, or that the binding constants at the two sites be identical. By this model, the ligand, Ca^{2+}, binds preferentially to the R state, and the myristoyl group functions as a built-in allosteric inhibitor, with higher affinity for the T state. Unmyristoylated recoverin, which is already in the R state (*23*), binds calcium at the two sites with very different affinities, which we take to be the instrinsic binding properties of the two sites. The X-ray structure of unmyristoylated recoverin with only a single Ca^{2+} bound in EF3 indicates that this is probably the higher affinity site, with a K_d of 0.11 μM, while EF2, by inference, is the lower affinity site, with a K_d of 6.9 μM. The cooperative binding to myristoylated protein is less tight than either, with an apparent K_d of 17.4 μM (*21*). Thus, part of the free energy of binding is used to drive the conformational change and to gain cooperativity.

Since removal of the myristate group increases the affinity for Ca^{2+} and eliminates the cooperativity of binding, we predicted that mutations decreasing the affinity of the protein for the myristoyl group in the Ca^{2+}-free state, or conversely favoring solvent interactions in the Ca^{2+}-bound state, ought to shift the allosteric equilibrium toward the R state, and increase the affinity for Ca^{2+}. In this paper, we describe two such mutants, W31K and I52A/Y53A. In the mutant W31K, in which Trp31 is replaced with Lys, we have introduced a side chain that favors solvent interactions; in mutant I52A/Y53A, we have replaced adjacent bulky side chains of Ile and Tyr with the smaller ones of Ala, thus diminishing the hydrophobic interactions that hold the myristoyl group in place in the T state. The effect of these changes on the Ca^{2+}-myristoyl switch is the subject of this paper.

MATERIALS AND METHODS

Mutagenesis. Recoverin mutants W31K and I52A/Y53A were prepared by means of the polymerase chain reaction overlap extension method (*24*) from the plasmid pTrec2 (*23*). After a two-step amplification, the mutant gene was restricted at a *Sac*I site just inside the start site, and at a *Bam*HI site in the 3′ polylinker, and was religated into pTrec2 from which the wild-type gene had been excised. The mutated gene was fully sequenced in each case by dideoxy termination, using Sequenase II from United States Biochemicals Corp.

Expression and Purification. The myristoylated mutant proteins were expressed in *E. coli* DH5$_\alpha$, cotransfected with the plasmid pBB131 (*25*), which contains the yeast myristoyl transferase gene, as described for the wild-type protein (*14*). The cells were grown at 32 °C, usually in Luria broth, as previously described (*23*). The myristoyl transferase was induced with IPTG,[1] and the recoverin by a temperature jump to 42 °C. The purification procedure was identical to that used for the wild-type protein. Briefly, after the cells were disrupted by sonication, the clarified extract was adsorbed to a Phenyl Sepharose column in the presence of high calcium and was eluted with buffer containing EGTA. After ion exchange chromatography on Q-Sepharose (Pharmacia),

[1] Abbreviations: *E. coli*, *Escherichia coli*; HPLC, high-performance liquid chromatography; HSQC, heteronuclear single quantum coherence; ROS, rod outer segment; DTT, DL-dithiothreitol; IPTG, isopropyl-thiogalactoside; EGTA, ethylene glycolbis(β-aminoethyl ether)-*N*,*N*,*N*′,*N*′-tetraacetic acid; 5,5′-dibromoBAPTA, 5,5′-dibromo-1,2-bis(*o*-aminophenoxy)ethane-*N*,*N*,*N*′,*N*′-tetraacetic acid; WT, wild type.

the resulting protein appeared homogeneous by gel electrophoresis and was more than 95% myristoylated as judged by HPLC on a Vydac C8 column. The structure was further confirmed by mass spectrometry.

Protein Concentration. Protein concentration was determined by the optical density at 280 nm, using for each protein a molar absorption coefficient calculated according to Pace et al. (26). For wild-type recoverin, $\epsilon = 23\,950\ cm^{-1}\ M^{-1}$; for W31K, $\epsilon = 18\,450\ cm^{-1}\ M^{-1}$, and for I52A/Y53A, $\epsilon = 22\,460\ cm^{-1}\ M^{-1}$.

Removal of Ca^{2+} from Buffers and Protein. The buffer routinely used for Ca^{2+} titrations was 50 mM HEPES, pH 7.5, containing 100 mM KCl and 1 mM DTT, from which Ca^{2+} was removed by passage through a 15 × 1 cm column of Chelex-100 (BioRad). The Ca^{2+} concentration in the sponged buffer was found to be 200 nM or less, based on the fluorescence of Fluo-3 (Molecular Probes) (*27*), using a K_d of 340 nM for Fluo-3. The protein itself was first passed over a Sephadex G-25 column prewashed with 1 mM EGTA followed by a large excess of Chelex-sponged buffer, and was then dialyzed overnight against a 500-fold excess of buffer, to remove EGTA. This turned out to be an important step, as even trace amounts of EGTA were found to affect the early points in a titration curve. The Sephadex-treated, dialyzed protein, in a volume of 1 mL, was then passed over a Chelex 100 column (1 g dry weight for myristoylated protein, 10 g dry weight for unmyristoylated protein) to remove contaminating Ca^{2+}. Fractions were collected in acid-washed microfuge tubes.

Ca^{2+} Standards. Stock solutions of $CaCl_2$ were prepared by volumetric dilution either of an Orion 0.1 M $CaCl_2$ standard solution or of a 0.1 M solution prepared by weighing $CaCl_2 \cdot 2H_2O$ (Sigma). Both sets of stock solutions gave identical results within the error of the experiment.

$^{45}Ca^{2+}$ Titrations. Direct titrations of Ca^{2+} binding were carried out by ultrafiltration in a Centricon-10 filtration unit (Amicon), as described by Ladant (*28*). To remove contaminating Ca^{2+} from the unit, the lower chamber was rinsed with acid and then with sponged buffer. The filter itself could not be treated with acid, but was decalcified by soaking it is 5% $NaHCO_3$ for at least 1 h, and then centrifuging it with sponged buffer at 6000 rpm until several milliliters of buffer had passed through the membrane. The relatively high concentration of protein (50 μM or higher in a total volume of 1.0 mL) made this assay fairly insensitive to Ca^{2+} contamination when myristoylated protein was titrated. On the other hand, it was difficult to establish the precise saturation level. The error bars increased dramatically once the binding sites on the protein had been filled, and $^{45}Ca^{2+}$ was being displaced by unlabeled Ca^{2+}. Contamination was important, however, in titrating unmyristoylated recoverin, whose high-affinity site is in the range of 0.1 μM.

Fluorescence Titrations. The conformational change which occurs when recoverin binds calcium was monitored by means of the tryptophan fluorescence. Since these titrations were done in the absence of Ca^{2+} buffers, and the protein concentration was low (1−2 μM), every effort was made to remove contaminating Ca^{2+}. The quartz cuvette and stirring bar were washed with 1 M HCl, and then rinsed extensively with sponged buffer to remove Ca^{2+}. Metal-free pipet tips were purchased from Applied Scientific. Titrations were carried out in 2.00 mL of Ca^{2+}-sponged HEPES, prepared as described above. Additions of $CaCl_2$ were made in 5−20 μL aliquots. Free Ca^{2+} concentrations were adjusted for the volume changes, and for the Ca^{2+} bound to protein, based on the relative change in fluorescence.

The Ca^{2+}-dependent change in tryptophan fluorescence emission was measured with an SLM 8000 scanning fluorimeter, using an excitation wavelength of 290 nm. Emission was monitored either at a single wavelength or by the integrated emission change above a filter cutoff of 335 nm. For the wild-type protein, which shows both a red shift and an increase in fluorescence on binding Ca^{2+}, the latter method gave the most sensitive measure of the change. This method, however, could not be used with the mutants. In particular, the Trp31 mutants showed a decreased fluorescent intensity rather than an increase, although they still displayed a small red shift on binding Ca^{2+}. For these mutants, the change above 335 nm was small, and the fluorescence emission was measured at a single wavelength (usually 324 nm), chosen for each mutant to maximize the observed change. The titration curve obtained was found to be independent of the wavelength chosen, with respect to the K_d and the Hill coefficient obtained. At the end of the titration, an excess of EGTA was added to the solution. Each measurement was normalized for the total change between the value at high Ca^{2+} and that in 1 mM EGTA. The close agreement between the EGTA point and the fluorescence of the first low calcium point in the titration showed that Ca^{2+} was effectively removed from the initial protein solution.

ROS Membranes. ROS membranes were prepared from commerically frozen retinas under dim light as described (*29*). The rhodopsin concentration was determined by measuring the absorption spectrum in 0.1% tetradecyltrimethylammonium bromide before and after bleaching, and subtracting the 500 nm absorbance of the bleached sample from the unbleached. A molar absorption coefficent of 40 600 $cm^{-1}\ M^{-1}$ was used to calculate the rhodopsin concentration. Unbleached membranes were flash-frozen in liguid nitrogen and stored in aliquots of 1 mL at −80 °C.

Preparation of Ca^{2+} Buffers. Whereas fluorescence and $^{45}Ca^{2+}$ titrations were performed without Ca^{2+} buffering, this was not possible in the ROS binding experiments. For these, 2 mM EGTA buffers, prepared as described by Tsien and Pozzan (*30*), were used below 0.5 μM free Ca^{2+}. Above 0.5 μM free Ca^{2+}, Ca^{2+} buffers were prepared from 2 mM 5,5′-dibromoBAPTA (Molecular Probes) by adding $CaCl_2$ directly. All buffers contained 50 mM HEPES, pH 7.5, and 100 mM KCl. The concentration of free calcium was assayed using an Orion Ca^{2+} electrode. In addition, the free Ca^{2+} in the EGTA buffers was determined by the fluorescence of Fluo-3. The two assays agreed to within about 25%.

Preparation of [^{3}H]Recoverin. E. coli $DH5_\alpha$ cells transfected with pTREC and pBB131 were grown in 100−250 mL cultures as usual. When the OD_{600} had reached 0.3, 1 mCi of [9,10-^{3}H]myristic acid (Amersham) in 1 mL of ethanol was added per 100 mL of culture. After induction of the myristoyl transferase and recoverin, the cells were harvested, and the extract was prepared as usual. The [^{3}H]-recoverin was purified on a 1 × 8 cm Phenyl Sepharose CL4B column (Pharmacia) followed by a 1 × 8 cm Q-Sepharose column which was eluted stepwise with 50 mM HEPES containing increasing amounts of KCl (0.05, 0.1, 0.15, 0.2, and 0.25 M). The fractions containing recoverin

were pooled, concentrated, and decalcified as usual. About $(15-20) \times 10^6$ cpm were recovered from an initial 2.5 mCi.

Ca^{2+}-Dependent Binding of Recoverin to ROS Membranes. Binding experiments were carried out as follows. An aliquot of ROS membranes was thawed at room temperature and then bleached for at least 15 min, until no further color change was seen by eye. It was aliquoted into 0.5 mL microfuge tubes so that the final concentration of rhodopsin would be 40−50 μM in a final volume of 125 μL. These aliquots were centrifuged at 10 000 rpm for 10 min, and the supernatant was removed. Each aliquot of membranes was then resuspended in 0.4 mL of one of the calcium buffers, and was vortexed for 10 s to break open the membranes. The samples were then centrifuged again, and the supernatant was discarded. Additional washes did not change the results of the titration. The packed volume of membranes in each sample was found to be about 15 μL. To this was added 100 μL of the appropriate calcium buffer, and 10 μL of [^{3}H]-recoverin, either wild type or mutant. The final concentration of recoverin was not precisely known, but was estimated to be about 0.02 μM. The samples were vortexed again, and were then incubated at room temperature with gentle shaking for at least 30 min. The samples were then transferred by pipet to cellulose propionate tubes (Robbins), and were centrifuged for 10 min in a Beckman airfuge set at 35 psi.

The supernatant was carefully removed and added directly to 5 mL of scintillation cocktail (CytoScint). Any remaining drops of supernatant were removed with the corner of a KimWipe. The pellet was resuspended in 100 μL of 5% Ammonyx Lo in water. It was found necessary to stir the pellet with the pipet tip, triturate it, and then allow it to sit in the detergent for about 30 min before transferring it to the scintillation fluid to guarantee that it was fully dissolved. Neither the calcium buffer nor 5% Ammonyx Lo quenched significantly in CytoScint (although some quenching was seen in EcoLume.) It was important, however, not to count the samples until all bubbles had cleared, and to have no particulate matter left in the sample. We were unable to eliminate completely the noise in these experiments. The error seems to result from a combination of factors, including the difficulty of handling small volumes, especially in the pipetting of the ROS membranes themselves, and possibly also from quenching of ^{3}H by rhodopsin.

In earlier experiments (14), the Ca^{2+} concentration was clamped by use of EGTA buffers. In the present experiments, the Ca^{2+} concentration above 0.5 μM was set with 5,5′-dibromoBAPTA (Molecular Probes), because this compound, with a K_d of 1.6 μM, buffers calcium well in the range of 0.5−10 μM (31).

NMR Spectroscopy. Recombinant myristoylated recoverin Wl31K and recoverin I52A/Y53A, uniformly labeled with ^{15}N, were expressed in *E. coli* DH5$_\alpha$F cotransfected with the appropriately mutated pTrec vector and pBB131. The bacteria were grown on minimal M9 medium (1) containing [^{15}N]ammonium chloride (Isotec, Inc., Miamisburg, OH). The protein was purified as described above. 2D ^{15}N−^{1}H HSQC experiments (*32*, *33*) were performed on a UNITY-plus 500 spectrometer, and the spectra were recorded using the enhanced sensitivity method of Kay et al. (*34*), with the numbers of points and acquisition times as described previously for the wild-type protein (*1*).

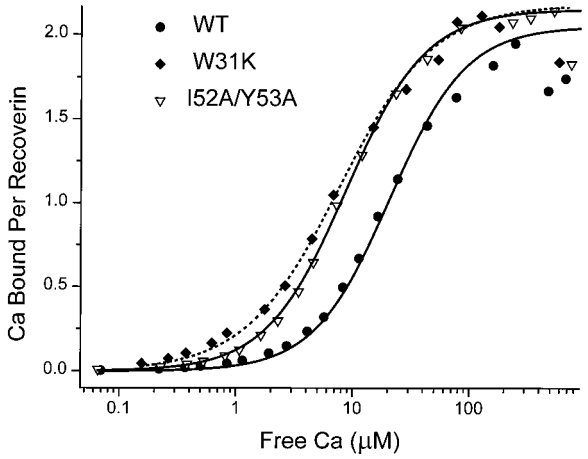

FIGURE 3: $^{45}Ca^{2+}$ titrations of wild-type recoverin (circles), recoverin W31K (diamonds), and recoverin I52A/Y53A (open triangles). Binding was determined by means of ultrafiltraton, as described Under Materials and Methods.

RESULTS

Binding of $^{45}Ca^{2+}$ to Recoverin. Titration of recoverin with $^{45}Ca^{2+}$ was carried out by ultrafiltration, according to the procedure of Ladant (*28*). Typical titration curves are shown in Figure 3. The curves saturate at two Ca^{2+} bound per protein, corresponding to the binding of Ca^{2+} to EF-2 and EF-3 (*15*, *21*). The binding data can be fit with the Hill equation:

$$Y = \frac{[Ca^{2+}]^\alpha}{[Ca^{2+}]^\alpha + K_d^\alpha} \quad (1)$$

with Hill coefficients (α) of 1.4 (wild type), 1.2 (W31K), and 1.3 (I52A/Y53A); and apparent dissociation constants (K_d) of 17.2 μM (wild type), 7.9 μM (W31K), and 8.1 μM (I52A/Y53A) (Table 1). The Hill coefficient of 1.4 indicates that the two Ca^{2+} bind cooperatively to myristoylated recoverin. For both mutants, the Hill coefficient is lower and the Ca^{2+} affinity is higher than those of wild type. The lower cooperativity and greater binding affinity of the mutants can be explained by a concerted allosteric model (*21*), a modification of the original model of Monod et al. (*22*). In the model depicted in Figure 2, recoverin has two *intrinsically* different binding sites for calcium and two protein conformational states, T and R. Let K_1 and K_2 denote the dissociation constants of the two sites (EF-3 and EF-2) in the R state. We assume that the conformational transition from R to T changes the binding constant of both sites by the same factor, *c*. *L* is the ratio of T/R in the absence of Ca^{2+}. The equilibria for this model are given by

$$K_1 = [Ca^{2+}]R_{00}/R_{01} = c[Ca^{2+}]T_{00}/T_{01} \quad (2)$$

$$K_2 = [Ca^{2+}]R_{01}/R_{11} = c[Ca^{2+}]T_{01}/T_{11} \quad (3)$$

$$L = T_{00}/R_{00} = T_{01}/cR_{01} = T_{11}/c^2R_{11} \quad (4)$$

where R_{ij} and T_{ij} represent recoverin in the R and T states, and the subscripts *i* and *j* denote whether Ca^{2+} is bound to

Table 1

	Hill equation		concerted model			
	K_d (μM)	α	L	K_1	K_2	c
			^{45}Ca Titrations[a]			
wild type	17.2 ± 1.3	1.4	379 ± 16.8	0.11	6.9	0.003
W31K	7.9 ± 1.5	1.2	61.1 ± 17.3	0.11	6.9	0.003
I52A/Y53A	8.1 ± 0.9	1.3	87.5 ± 17.7	0.11	6.9	0.003
			Fluorescence Titrations[b]			
wild type	17.9 ± 1.0	1.4	387.6 ± 33	0.11	6.9	0.003
W31K	3.6 ± 0.2	1.2	50.7 ± 4.1	0.11	6.9	0.003
I52A/Y53A	4.4 ± 0.5	1.0	73.5 ± 4.4	0.11	6.9	0.003
			ROS Binding[c]			
wild type	5.6 ± 1.0	1.4 ± 0.3				
W31K	2.2 ± 0.7	1.2 ± 0.3				
I52A/Y53A	1.0 ± 0.3	1.1 ± 0.1				

[a] Parameters obtained by fitting the $^{45}Ca^{2+}$ binding data to the Hill equation and to the allosteric equation for the fractional saturation of binding sites, Y (eq 6 in the text). α is the Hill coefficient. In fitting the concerted model, the intrinsic binding constants K_1 and K_2 (μM) for the two sites were held constant, equal to the values previously obtained for wild-type recoverin by flow dialysis (*21*). The constant c was first optimized as described in the text, and then held constant. Error indicates the standard deviation between three or more experiments. [b] Parameters obtained by fitting the fluorescence titration data for recoverin and the two mutants to the Hill equation and to the allosteric equation for the fractional occupancy of the R state, F (eq 9). [c] Parameters obtained by fitting the ROS binding data to the Hill equation. For each protein, the data from three experiments were fitted as a single curve. This was done, rather than fitting the mean, to include as many data points as possible, because different buffer sets were used for some of the experiments.

the low-affinity (EF-2) and high-affinity (EF-3) sites, respectively. The fractional saturation, Y, is

$$Y = 0.5(R_{01} + T_{01} + 2R_{11} + 2T_{11})/(R_{00} + T_{00} + R_{01} + T_{01} + R_{11} + T_{11}) \quad (5)$$

The dependence of Y on $[Ca^{2+}]$ is given by

$$Y = 0.5\left(\frac{\beta\frac{[Ca^{2+}]}{K_1} + 2\gamma\frac{[Ca^{2+}]^2}{K_1K_2}}{1 + L^{-1} + \beta\frac{[Ca^{2+}]}{K_1} + \gamma\frac{[Ca^{2+}]^2}{K_1K_2}}\right) \quad (6)$$

where $\beta = c + L^{-1}$ and $\gamma = c^2 + L^{-1}$. The dissociation constants of the R state are taken to be equal to the microscopic dissociation constants measured from the binding data of unmyristoylated recoverin (*21*). This approximation is likely to be valid because of the 70-fold difference between the two measured constants, and because two lines of evidence indicate that unmyristoylated wild-type recoverin is in the R state, or very close to the R state, even without bound Ca^{2+}. First, the tryptophan fluorescence spectrum of unmyristoylated wild-type recoverin in both Ca^{2+}-free and Ca^{2+}-bound states closely resembles that of myristoylated Ca^{2+}-bound recoverin (i.e., the R state) (*23*, *35*). The spectrum of each of the two mutants when the protein is unmyristoylated and Ca^{2+}-free is likewise indistinguishable from that of the R state (data not shown).

Second, there is NMR evidence to suggest that unmyristoylated recoverin occupies the R state in both the Ca^{2+}-free and Ca^{2+}-bound states. We determined the structure of

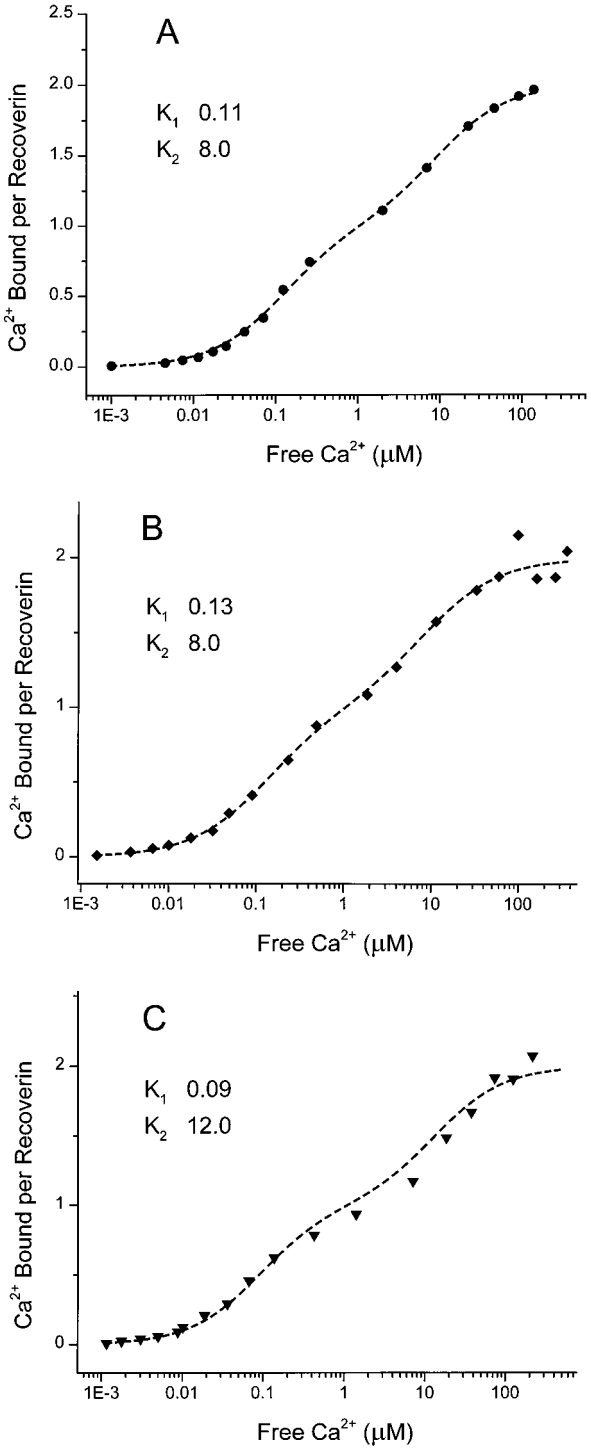

FIGURE 4: $^{45}Ca^{2+}$ titration of unmyristoylated WT recoverin (panel A), recoverin W31K (panel B), and recoverin I52A/Y53A (panel C). For each protein, K_1 and K_2 were obtained by fitting the data with eq 7.

unmyristoylated recoverin with two Ca^{2+} bound by NMR (*35*) to be nearly identical to the X-ray structure of recoverin with one Ca^{2+} bound (*15*). In addition, the amide proton and ^{15}N chemical shifts of unmyristoylated wild-type recoverin in the Ca^{2+}-free state match, within experimental error, the resonance frequencies observed for Ca^{2+}-bound myristoylated recoverin, and do not change much during a Ca^{2+} titration. In contrast, large chemical shift differences are observed between the Ca^{2+}-free (T state) and Ca^{2+}-bound (R state) states of myristoylated wild-type recoverin.

In the $^{45}Ca^{2+}$ titrations, the error in the concentration of bound Ca^{2+} (vertical dimension) greatly increases as saturation is approached because it is calculated as a small difference between two large numbers: the total and free Ca^{2+} concentrations. It is therefore difficult to determine accurately the saturation level. Small errors in the concentration of bound Ca^{2+} do not have a large effect on the value of *L*, but affect profoundly the value of *c*. Therefore, each data set was fitted to a modified version of eq 6, containing a scaling factor *n*, which was initially allowed to float (along with *L*), while *c* was fixed at an arbitrary level. The value of *n*, which varied from 0.98 to 1.02, was then fixed and *c* allowed to float. Fitting cycles were repeated until convergence was reached. For wild-type protein, the average value for *L* obtained by this procedure, using 5 separate data sets, was 379.2 ± 16.8 (4.4%), fitting error = 13.4, $\chi^2 = 0.001$, and the average value of *c* was 0.00283 ± 0.00051 (18.0%), fitting error = 0.00044 (16%). The values of *c* obtained in this way for the mutant proteins (0.00346 ± 26% for I52A/Y53A, and 0.00527 ± 34% for W31K) were less consistent, and could vary by as much as 2-fold, depending on how many of the last data points were included in the fit. We therefore rounded off the wild-type value of c to 0.003, and assumed it to be unchanged in the mutants (Table 1). It is undoubtedly an oversimplification, especially for W31K, for which *c* may be somewhat higher than for wild type, but seems prudent since this difference is not much greater than the error between multiple experiments. Moreover, the effect on *L* is small: when *c* is taken as 0.00527, *L* is calculated for W31K to be 64, compared to 61 when *c* is taken as 0.003. The mutant titration data are well fit by the model, with *L* lower for the mutants than for the wild type. In contrast, if *L* is fixed at the wild-type value of 379, and *c* allowed to float, the data for the mutants cannot be fit, as *c* reflects the steepness of the curve, but not the shift in K_d. Thus, we believe the qualitative conclusions are valid even without a reliable value of *c*. Our estimate of *c* is similar to that found in other allosteric proteins (*22*). We have no means of separating *c* for the two sites, and thus use an average value. This analysis reveals that the higher binding affinity and lower cooperativity of the mutants relative to the wildltype can be explained by a lowering of *L*, keeping all other parameters fixed.

To test our assumption that the intrinsic binding constants of the two sites are not significantly affected by the mutations, we titrated unmyristoylated versions of wild-type recoverin and the two mutants by ultrafiltration. Biphasic curves were obtained for all three proteins (Figure 4). The curves were fit with the Hill equation for two independent sites:

$$Y = 0.5\left(\frac{[Ca^{2+}]_f}{[Ca^{2+}]_f + K_1} + \frac{[Ca^{2+}]_f}{[Ca^{2+}]_f + K_2}\right) \qquad (7)$$

The values for the dissociation constants K_1 and K_2 obtained for the wild-type and mutant proteins are shown on the graphs of Figure 4. The values of 0.11 ± 0.02 and 8.0 ± 1.0 μM for the wild-type protein are in good agreement with the earlier values of 0.11 and 6.9 μM obtained by flow dialysis. Mutant W31K displayed values of K_1 and K_2 indistinguishable from those of WT, within the error of the measurement. The high-affinity site of mutant I52A/Y53A titrated at 0.09 μM, within experimental error of the WT value; the lower affinity site, with a K_d of 12 μM, appeared to have slightly lower affinity that that of WT. Clearly, the small change in the intrinsic K_d cannot account for the increased affinity of the myristoylated protein because it is in the opposite direction. Therefore, our assumption that the binding sites themselves are basically unchanged by these mutations gives an upper limit for the true value of *L* in each case. The simplest interpretation of the binding data for myristoylated protein is that the mutations primarily shift the allosteric equilibrium toward the R state, most likely by destabilizing the T state.

Ca^{2+} Dependence of Conformational Change. The fluorescence emission spectra of wild-type, W31K, and I52A/Y53A recoverin in high and low Ca^{2+} are shown in Figure 5. Wild-type recoverin shows both a red shift and an increase in fluorescence intensity on binding Ca^{2+} (Figure 5A), as previously reported (*35*). The mutant W31K, on the other hand, shows a large decrease in fluorescence intensity and a small red shift in emission (Figure 5B). A similar change is seen with mutant W31E, and with W31F (data not shown). There are three tryptophan residues (Trp31, Trp104, and Trp156) in recoverin that account for the intrinsic fluorescence. From the structures of recoverin, Trp31 is buried near the myristoyl group in the Ca^{2+}-free state and is solvent-exposed in the Ca^{2+}-bound state. Prior mutagenesis studies indicate that the emission intensity due to Trp31 of recoverin increases more than 10-fold on binding Ca^{2+} (Trager et al., unpublished results). In Trp31 mutants, in which the emission spectrum reflects the fluorescence of Trp104 and Trp156 alone, the observed intensity is lower in the Ca^{2+}-bound state than in the Ca^{2+}-free state. The spectral change of I52A/Y53A more closely resembles that of wild-type recoverin, showing a red shift and only a slight decrease in fluorescence intensity in going from the Ca^{2+}-free to the Ca^{2+}-bound state (Figure 5C).

The change in tryptophan fluorescence on binding Ca^{2+} was used to monitor the Ca^{2+}-dependent conformational changes. Typical Ca^{2+} titration curves for wild-type myristoylated recoverin and the two mutants are shown in Figure 6. The midpoint of the titration was shifted to lower Ca^{2+} concentrations for both of the mutants relative to wild type. The same was true for two other mutants of the myristoyl binding pocket, W31E and L90K (data not shown). When the fluorescence titration data were fit with the Hill equation, the Hill coefficient was calculated to be 1.4 (wild type), 1.2 (W31K), and 1.0 (I52A/Y53A), and the midpoint of the change occurred at 17.9 μM (wild type), 3.6 μM (W31K), and 4.4 μM (I52A/Y53A) free Ca^{2+} (Table 1). For the wild-type protein, the midpoint of the fluorescence titration agreed well with the apparent K_d obtained by $^{45}Ca^{2+}$ binding data. For both mutants, the midpoint of the fluorescence titration occurred at Ca^{2+} concentrations (3.6 and 4.4 μM) that were lower than the apparent K_d measured from the $^{45}Ca^{2+}$ binding curves.

In the fluorescence titrations, the end point is well-defined, but the initial Ca^{2+} concentration at the start of the titration is less certain due to Ca^{2+} contamination from the glassware. This contamination was minimized and estimated to be less than 200 nM based on fluorescence measurements using the Ca^{2+} indicator dye Fluo-3 (*27*). Also, the initial tryptophan

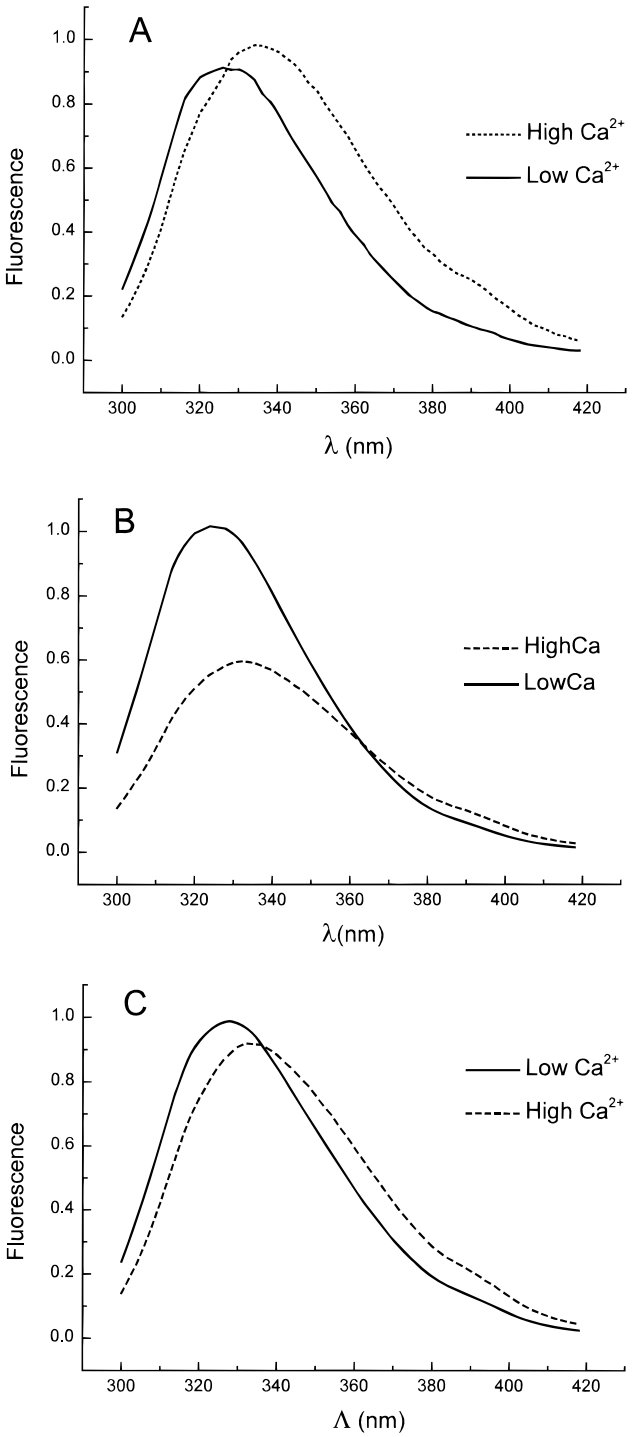

FIGURE 5: Fluorescence emission spectra of wild-type recoverin (panel A), recoverin W31K (panel B), and recoverin I52A/Y53A (panel C), in low and high Ca^{2+}.

fluorescence at the start of the titration was compared to that after the addition of excess EGTA ($[Ca^{2+}]_{free}$ less than 10 nM) at the end of the titration. Typically, the difference in fluorescence was less than 5% of the total, indicating that more than 95% of the protein was titrated.

The change in fluorescence monitors directly the change in environment of the tryptophan residues. A priori, we do not know whether this reflects the global conformational change, or the binding of Ca^{2+} per se. Trp104 is adjacent to the EF3 binding loop, and might respond to the presence of the first bound Ca^{2+}. This might explain why the decrease

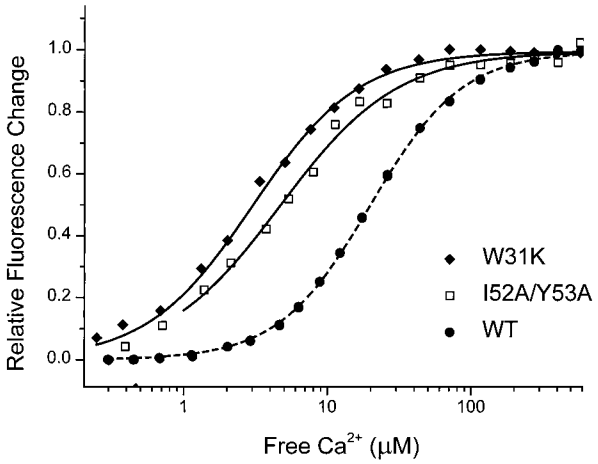

FIGURE 6: Change in protein conformation of WT recoverin (filled circles), recoverin W31K (closed diamonds), and recoverin I52A/Y53A (open squares), measured by the relative change in fluorescence emission.

in fluorescence of mutant W31K would precede the saturation of Ca^{2+} sites with respect to Ca^{2+} concentration. The same argument cannot be applied to mutant I52A/Y53A, however, since Trp31 is still present in this mutant. We propose instead that the change in fluorescence in both mutants, as well as the wild-type protein, reflects the change from the T to the R state. This seems justified because we know from the NMR structures of the wild-type protein that a large conformational change occurs, and that both Trp31 and Trp104 are located in regions of structural change. Moreover, we show below that the fluorescence titrations can be fit by an equation for the fractional occupancy of the R state, and yield values of L (Table 1) that match those obtained by $^{45}Ca^{2+}$ titration, as predicted by the concerted allosteric model.

The expression for the fractional saturation of the Ca^{2+} binding sites was given in eq 5. The fractional occupancy of the R state is defined as

$$F = (R_{00} + R_{01} + R_{11})/(R_{00} + T_{00} + R_{01} + T_{01} + R_{11} + T_{11}) \quad (8)$$

which, as a function of Ca^{2+} concentration, becomes

$$F = \frac{L^{-1} + \frac{[Ca^{2+}]}{LK_1} + \frac{[Ca^{2+}]^2}{LK_1K_2}}{1 + L^{-1} + \frac{\beta[Ca^{2+}]}{K_1} + \frac{\gamma[Ca^{2+}]^2}{K_1K_2}} \quad (9)$$

On fitting the data with F, and allowing both L and c to float, the average L for WT recoverin was found to be 396.9 ± 38.5 (fitting error = 17.7, $\chi^2 = 0.0018$), and c was 0.00254 ± 0.00045 (fitting error = 0.00033). For mutant W31K, L was calculated to be 40.1 ± 5.6 (fitting error = 2.76, $\chi^2 = 0.00070$), and c was 0.00578 ± 0.0012 (fitting error, 0.0016). For mutant I52A/Y53A, the average L was 62.9 ± 11.2 (fitting error = 6.59, $\chi^2 = 0.00096$), and c was 0.00233 (fitting error = 0.001). Once again, we refitted the data holding c fixed at 0.003. This had the effect of changing the values of L to those shown in Table 1 (WT, 387.6; W31K, 50.7; I52A/Y53A, 73.5) and reducing the fitting error by a

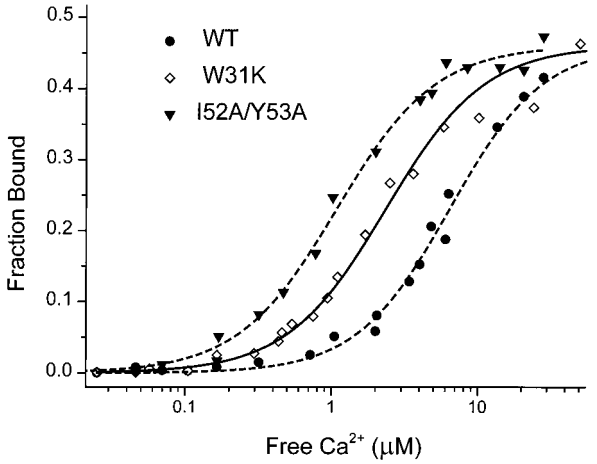

FIGURE 7: Binding of tritiated WT recoverin (filled circles), recoverin W31K (open squares), and recoverin I52A/Y53A (filled triangles) to ROS membranes, as described Under Materials and Methods. Each curve represents an individual experiment.

factor of 2. The values of *L* calculated by fitting the fluorescence data with *F* are in good agreement with those obtained by fitting the Ca^{2+} binding data with *Y* (Table 1).

From eqs 5 and 8, we can see that *F* equals *Y* in the limit where the equilibrium species R_{00}, R_{01}, T_{01}, and T_{11} have zero or low concentration compared to the species without Ca^{2+} (T_{00}) and with two Ca^{2+} bound (R_{11}), that is, when the binding of two Ca^{2+} is highly cooperative. For wild-type recoverin, the binding of two Ca^{2+} is cooperative ($\alpha = 1.4$); modeling shows that the fraction of species with one Ca^{2+} bound never exceeds 20% of the total. Hence, the fluorescence titration curve nearly superimposes with the fractional saturation curve. For both mutants, the cooperativity is lower ($\alpha = 1.2$ for W31K, 1.0 for I52A/Y53A) and the fraction of species with one Ca^{2+} bound approaches 40% of the total. The high fraction of species with one Ca^{2+} bound leads to the observed difference between the fluorescence titration and the fractional binding curves, and suggests that the binding of a single Ca^{2+} may be sufficient to drive the allosteric transition in the mutants.

Binding of [^{3}H]Recoverin to ROS Membranes. It had previously been shown that myristoylated recoverin binds to ROS membranes in a calcium-dependent way, and that the myristoyl group itself is required for this interaction (*14*). Using this assay, the calcium dependence of binding by the two mutants was compared to that of wild-type recoverin (Figure 7). The data were fit with the Hill equation (Table 1). Both mutants bound to membranes at a lower [Ca^{2+}] than did the wild-type protein (WT, 5.6 ± 1.0 μM; W31K, 2.2 ± 0.7 μM; I52A/Y53A, 1.0 ± 0.3 μM). R_{00}, R_{01}, and R_{11} all contribute to the observed membrane binding, to the extent to which they are populated. The Ca^{2+} dependence of membrane binding is therefore more closely related to the fractional occupancy of the R state, *F*, than to the fractional saturation of Ca^{2+} binding sites, *Y*. The ratio of the K_d measured by fluorescence change to the $K_{1/2}$ determined for membrane binding provides a measure of the effect of membranes on the various equilibria between the T and R states. This ratio is 3.2 for WT, 1.6 for W31K, and 4.4 for I52A/Y53A. The difference between these numbers probably reflects the intrinsic error of the membrane binding experiment.

The $K_{1/2}$ of 5.6 μM reported here for the fractional binding of wild-type [^{3}H]recoverin as a function of free [Ca^{2+}] is higher than the 2.2 μM previously reported (*14*). The Ca^{2+} dependence is also less cooperative (Hill coefficient of 1.4 as opposed to 2.38). These differences seem to result from using 5,5′-dibromoBAPTA instead of EGTA to set the Ca^{2+} levels above 0.5 μM free Ca^{2+}. Indeed, when EGTA buffers were used, the binding curve rose more steeply. Thus, the EGTA buffers failed to hold the free Ca^{2+} levels in this range after the addition of ROS membranes. The various difficulties involved in setting the calcium level accurately have already been discussed at some length by Calvert et al. (*7*), and we confirm their conclusions.

Two-Dimensional NMR Spectra. To probe structural changes induced by the mutations, two-dimensional ^{15}N−^{1}H HSQC spectra of the Ca^{2+}-free, myristoylated forms of W31K and I52A/Y53A were measured and compared to that of wild-type (Figure 8). The cross-peaks in the spectra represent amide proton resonances. Sequence-specific resonance assignments of wild-type recoverin have been obtained previously (*1*). The assigned peaks in Figure 8A serve as fingerprints of the conformation of the main chain and side chain amide groups. The spectra of the mutants are quite similar to the wild-type spectrum, suggesting that the overall backbone structure is not greatly perturbed in the mutants. The spectrum of W31K does not exhibit the cross-peak assigned to the side chain indole proton of Trp31, thus confirming that Trp31 has been mutated. Also, the peaks representing the backbone amide protons of the mutated residues (Trp31, Ile52, and Tyr53) are found to be shifted in the mutant spectra as expected.

The ^{15}N and ^{1}H chemical shifts of the resonances in the mutant spectra were quantitatively compared to the full set of assigned chemical shifts of the wild-type spectrum. If the ^{1}H and ^{15}N chemical shifts of a given mutant peak were within 0.04 and 0.15 ppm, respectively, of a wild-type peak, then the two peaks were defined as matched. A total of 73 and 63 matches were observed for peaks in the spectra of W31K and I52A/Y53A, respectively (Table 2). Peaks in the wild-type spectrum that are assigned to more than one residue due to spectral overlap were not considered and were defined as overlapped peaks. A total of 66 peaks were identified as overlapped in the wild-type spectrum (Table 2). In addition, five peaks from the W31K spectrum and six peaks from the I52A/Y53A spectrum were disqualified as matches due to the low signal-to-noise ratio, and were not counted in the totals. Peaks that were neither overlapped nor matched were defined as shifted peaks. A total of 50 and 59 peaks were classified as shifted in the spectra of W31K and I52A/Y53A, respectively (Table 2).

Most of the matches were identified as peaks of the C-terminal domain. The large number of matched peaks of this domain strongly suggests that its backbone structure in both mutants is nearly identical to that of wild type. Moreover, within this domain, most of the peaks associated with the Ca^{2+}-binding loop of EF-3 in the wild-type spectrum were matched by corresponding resonances in the mutant spectra (D110, D112, G113, N114, G115, T116, K119, N120, and E121 in the W31K spectrum; and D112, G113, T116, K119, N120, and E121 in the I52A/Y53A spectrum). This is strong evidence that this site is structurally intact and has not been disabled by either mutation. In contrast,

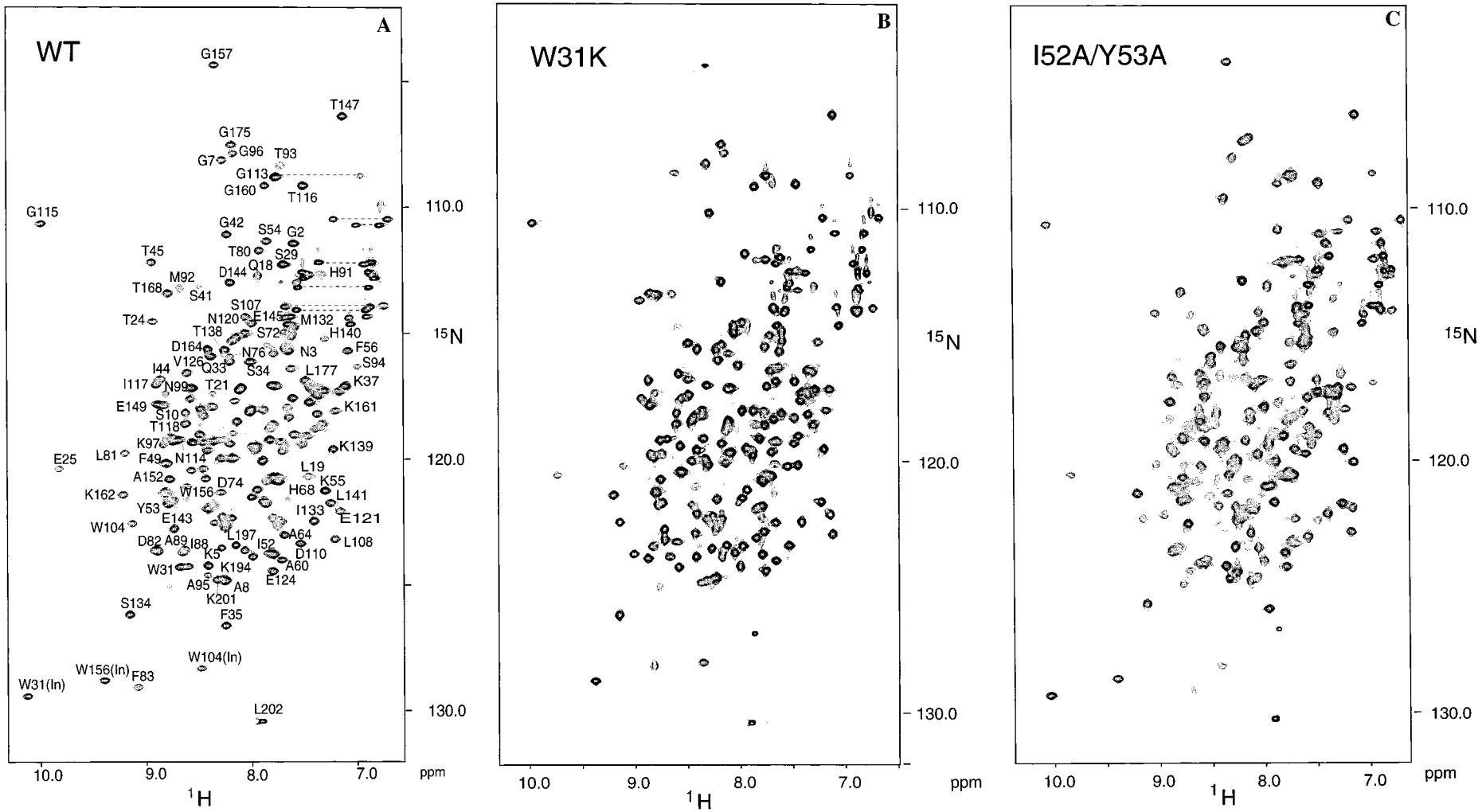

FIGURE 8: 2D $^{15}N-^{1}H$ HSQC spectrum of WT Ca^{2+}-free myristoylated recoverin, with assignments from Ames et al. (*1*) (panel A), mutant W31K (panel B), and mutant I52A/Y53A (panel C).

Table 2: Comparison of Mutant $^1H-^{15}N$ Resonances with Those of Wild Type[a]

mutant	domain	matched with WT	shifted in mutants	overlapped in WT	total
W31K	N-term	18 (19%)	45 (47%)	33	96
	C-term	55 (59%)	5 (5.4%)	33	93
I52A/Y53A	N-term	12 (13%)	48 (52%)	33	93
	C-term	51 (54%)	11 (12%)	33	95

[a] Quantitative comparison of the ^1H and ^{15}N resonances of W31K and I52A/Y53A with those of wild-type recoverin in the Ca^{2+}-free state. Matched peaks are defined as having ^1H and ^{15}N shifts within 0.04 and 0.15 ppm, respectively, of the corresponding peaks of wild type, as in Figure 8. Overlapped peaks refer to peaks in the wild-type 2D spectrum to which more than one amide proton has been assigned (*1*). Shifted peaks are those from the wild-type assignments for which there is no match in the mutant spectrum, and which are not overlapped in the wild-type spectrum. Total refers to the total WT peaks analyzed, minus five W31K peaks and six I52A/Y53A peaks that were ambiguous in the mutant spectra. Percentage refers to the percent of the peaks from each domain, based on the total number given in the table.

there are many more shifts in the N-terminal domain, suggesting that there might be backbone adjustment in the region of the mutations, as described in cavity-creating mutants of T4 lysozyme (*37*), but without residue assignments and NOE data, the extent of these changes is unclear.

DISCUSSION

The goal of this study was to analyze the effect of core mutations on the allosteric properties of recoverin. Mutation of hydrophobic core residues (Trp31, Ileu52, and Tyr53) causes an increase in the Ca^{2+}-binding affinity accompanied by a decrease in cooperativity. These observations are best explained by a shift of the allosteric equilibrium between the Ca^{2+}-free form, in which the myristoyl group is sequestered, and the Ca^{2+}-bound form, in which the myristoyl group is extruded, without affecting the intrinsic binding constants for the two Ca^{2+} sites. This analysis reveals that mutations in the hydrophobic core can fine-tune the range of Ca^{2+} concentrations needed to drive a $Ca^{2+}-$myristoyl switch, and might be used for engineering Ca^{2+} sensors with different Ca^{2+} affinities.

Cooperativity of Binding. In the present set of binding experiments, we have consistently observed a Hill coefficient of 1.4 for wild-type myristoylated recoverin instead of the previously reported 1.7 (*21*). We do not fully understand this difference. In the fluorescence titration, we have been able to show that the higher Hill coefficient observed in earlier experiments was due to incomplete removal of EGTA from the protein sample used for the tiration. The titration looks sharper in the presence of contaminating EGTA because the true free Ca^{2+} concentration is lower than calculated. This affects the beginning of the titration, but is insignificant at higher Ca^{2+} levels. EGTA might account for the higher Hill coefficient observed in the original flow dialysis experiments if the $Ca^{2+}-$EGTA complex diffused through the membrane, increasing the apparent free Ca^{2+} concentration. Conversely, if it were retained, the EGTA contamination should lower the Hill coefficient in the flow dialysis experiments by superimposing a second titration at low Ca^{2+} levels. We have not resolved this issue. We nonetheless now believe that the consistency between the recent $^{45}Ca^{2+}$ binding data, obtained using the ultrafiltration technique, and the fluorescence titration supports our contention that a Hill coefficient of 1.4 is probably more correct for wild-type recoverin. Fitting the binding curves with the concerted model gives a *c* value of 0.003, compared to 0.0001 previously calculated. The newer value of *c*, reflecting a 333-fold binding preference of Ca^{2+} for the R state over the T state, is more comparable to *c* values of other allosteric proteins, such as hemoglobin, with a *c* of 0.014 (*22*).

The lower value of the Hill coefficient does not change the qualitative picture of cooperativity of binding. In oligomeric allosteric proteins that display symmetrical homotropic binding, the lower limit for the Hill coefficient, in the noncooperative case, is 1. Recoverin is not symmetrical, however. The two binding sites display widely different intrinsic binding properties when titrated in unmyristoylated wild-type protein. The biphasic titration curve has a slope of only 0.4 at its midpoint. Thus, the lower bound for the Hill coefficient is 0.4 in this system, and a Hill coefficient of 1.0 is therefore significantly cooperative.

Several reports indicate that inhibition of rhodopsin kinase by recoverin is also highly cooperative with respect to Ca^{2+} (*7*−*9*). Calvert and Chen both used 5,5′-dibromoBAPTA to set the Ca^{2+} levels in their kinase assays, so this cooperativity is undoubtedly *not* an artifact of Ca^{2+} buffering. Possibly the kinase not only stabilizes the R form of recoverin but also alters the intrinsic binding properties of one of the EF hands for Ca^{2+}, in a way that would enhance cooperativity. EF-2 has an unusually low affinity for Ca^{2+} due to its somewhat strained conformation. Interaction of the kinase might somehow relieve this strain. It will be of interest to test the cooperativity of our allosteric mutants in their direct effect on rhodopsin kinase activity, since the increased affinity for Ca^{2+} would be expected to lower the Ca^{2+} concentration at which half-maximal kinase inhibition is seen while perhaps lowering the cooperativity relative to wild type.

Fractional Ligand Saturation and Occupancy of the R State. It was long ago recognized that the fractional conformational change of an allosteric protein can precede fractional saturation with ligand. This is a direct consequence of the difference between the two equations for *Y* and *F* discussed above. For example, in aspartate transcarbamylase, a complex of six catalytic and six regulatory subunits, it was shown that the fractional change in sedimentation rate of the reconstituted oligomeric enzyme occurred at a lower concentration of the substrate succinate than did the occupancy of succinate binding sites (*38*, *39*). In the present system, we have seen that the global conformational change of the two mutants, monitored by fractional change in tryptophan fluorescence, likewise occurs at a lower Ca^{2+} concentration than the corresponding fractional saturation of binding sites, measured directly by $^{45}Ca^{2+}$ binding. This is exactly what one expects when the two sites have very different affinities and when the binding of a single Ca^{2+} can increase the probability of the transition from the T to the R state. This effect is masked when the ratio of T_0/R_0 is high, making the transition highly cooperative, as in wild-type recoverin, but is seen for both mutants, which display lower cooperativity.

Effect of ROS Membranes on the Conformational Change. Recoverin binds to ROS membranes only when it is myristoylated and Ca^{2+}-bound (*14*). Insertion of the fatty acyl

group into the lipid bilayer is believed to be the primary interaction of the myristoylated protein with the membrane, since synthetic lipid micelles can also function as receptors. Transfer of the myristoyl group to the lipophilic environment of the membrane lowers the free energy required to extrude it from the protein core. Membranes would therefore be expected to lower the ratio of T_0/R_0. This idea is consistent with our observation that the free [Ca^{2+}] at which half-maximal membrane binding occurs is lower than the K_d for the binding of Ca^{2+} to recoverin, or for the conformational change associated with binding, in the absence of membranes. Even when the T_0/R_0 ratio has already been lowered by the presence of a core mutation that makes the T_0 state less energetically favorable, the membrane interaction further drives the conformational change.

Comparison with Mutants of Troponin C and Calbindin. Mutants of troponin C that increase the affinity for Ca^{2+} at the two low-affinity sites within the N-terminal domain of that protein have also been reported (*40*). Like recoverin, troponin C has four EF-hand motifs (*11*). In that protein, however, all four sites bind Ca^{2+}. There is a large difference in affinity for Ca^{2+} between the N-terminal domain and the C-terminal domain, but there is no cooperativity between the two domains, which are separated by a rigid α-helical linker. Binding of Ca^{2+} to the two low-affinity N-terminal sites does, however, result in a conformational change, more limited in scope than the change seen in recoverin. In both proteins, hydrophobic residues within the core become solvent-exposed (in the absence of effector proteins). As in recoverin, mutation of these hydrophobic residues in troponin C to more polar ones pulls the equilibrium toward the Ca^{2+}-bound state (*40*−*42*).

A mutant of calbindin D_{9k}, namely, P43MG, also shows increased affinity for Ca^{2+} relative to the wild type (*43*). This mutant, in the Ca^{2+}-bound state, appears to contain a new short helical segment in the tether region between the two EF-hands, which presumably stabilizes the conformation of the helices entering and exiting the binding loops. The mutations we have made in recoverin appear to function differently. The three targeted residues are all located on existing helices. The relatively small changes in the HSQC spectra suggest that no major backbone change has occurred. In addition, preliminary urea denaturation curves, measured by circular dichroism, reveal small decreases in stability of both mutants relative to wild type. As expected, the shift is greater in the Ca^{2+}-free state than the Ca^{2+}-bound state (A. N. Baldwin, unpublished results), consistent with a decrease in the ratio of T_0/R_0 if the fully denatured state is the same with or without Ca^{2+}. The change in T_m between mutants and wild type is very small relative to the overall stabilization of secondary structure by Ca^{2+}. Quantitative conclusions cannot be drawn, however, because the urea denaturation does not appear to be a two-state transition.

Conservation of the Myristoyl Binding Pocket. The binding pocket for the myristoyl group in the T state is highly conserved among proteins of this family, if one looks at those residues in Ca^{2+}-free wild-type recoverin located less than 5 Å from the myristoyl group (*13*). This suggests that the myristoyl switch has evolved to meet very specific functional requirements. Assuming that the basic four EF-hand fold evolved by gene duplication (*44*), the addition of the myristoyl group as an allosteric effector probably came later. The strength of the inhibition is capable of fine-tuning the protein's response to Ca^{2+}, and thus setting the conformational switch, although most proteins in this family have not diverged enough to display this. GCAP1 (*45*) and GCAP2 (*46*) have both replaced Ileu52 and Tyr53 of recoverin with two Phe, but at least in GCAP2 the myristoyl group does not appear to function as a switch (*47*). In any case, the mutations probably do not account for the lower K_d of these proteins, whose conformational change, like that of neurocalcin and hippocalcin, is driven by the binding of three Ca^{2+} ions.

Characterization of core mutants of recoverin with increased affinity for Ca^{2+} adds further support for the allosteric model we have used to describe the conformational states of the wild-type protein. By this model, the myristoyl group acts as a built-in allosteric inhibitor, which keeps the protein in the T conformation in the Ca^{2+}-free state, decreases the affinity for Ca^{2+}, and results in a cooperative transition on binding Ca^{2+}.

ACKNOWLEDGMENT

We thank Dr. Lubert Stryer for his ongoing support in carrying out these experiments and in reviewing the manuscript. We also gratefully acknowledge the use of the NMR facilities under the direction of Dr. Mitsu Ikura in performing the HSQC experiments, and thank Dr. Tom Neubert for confirming the mass of the mutant proteins by mass spectrometry at the University of Washington.

REFERENCES

1. Ames, J. B., Tanaka, T., Stryer, L., and Ikura, M. (1994) *Biochemistry 33*, 10743−10753.
2. Gray-Keller, M. P., Polans, A. S., Palczewski, K., and Detwiler, P. B. (1993) *Neuron 10*, 523−531.
3. Erikson, M. A., Lagnado, L., Zozula, S., Neubert, T. A., Stryer, L., and Baylor, D. A. (1998) *Proc. Natl. Acad. Sci. U.S.A. 95*, 6374−6479.
4. Dodd, R. L., Makino, C. L., Chen, J., Simon, M. I., and Baylor, D. A. (1995) *Invest. Ophthalmol. Visual Sci. 36*, S641.
5. Dodd, R. L. (1998) Thesis, Stanford University, Palo Alto, CA.
6. Kawamura, S., Cox, J. A., and Nef, P. (1994) *Biochem. Biophys. Res. Commun. 203*, 121−127.
7. Calvert, P., Klenchin, V. A., and Bownds, M. D. (1995) *J. Biol. Chem. 270*, 24127−24129.
8. Klenchin, V. A., Calvert, P. D., and Bownds, M. D. (1995) *J. Biol. Chem. 270*, 16147−16152.
9. Chen, C.-K., Inglese, J., Lefkowitz, R. J., and Hurley, J. B. (1995) *J. Biol. Chem. 270*, 18060−18066.
10. Kretzinger, R. H., and Nockolds, C. E. (1993) *J. Biol. Chem. 248*, 3313−3326.
11. Herzberg, O., and James, M. N. G. (1985) *Nature 313*, 653−659.
12. Babu, Y. S., Sack, J. S., Greenbough, T. J., Bugg, C. E., Means, A. R., and Cook, W. J. (1985) *Nature 315*, 37−40.
13. Tanaka, T., Ames, J. B., Harvey, T. S., Stryer, L., and Ikura, M. (1995) *Nature 376*, 444−447.
14. Zozulya, S., and Stryer, L. (1992) *Proc. Natl. Acad. Sci. U.S.A. 89*, 11569−11573.
15. Flaherty, K. M., Zozulya, S., Stryer, L., and McKay, D. B. (1993) *Cell 75*, 709−716.
16. Kuno, T., Kajimoto, Y., Hashimoto, T., Shirai, Y., Saheki, S., and Tanaka, T. (1992) *Biochem. Biophys. Res. Commun. 184*, 1219−1225.
17. Nakano, A., Terasawa, M., Watanabe, M., Usuda, N., Morita, T., and Hidaka, H. (1992) *Biochem. Biophys. Res. Commun. 186*, 1207−1211.

18. Kobayashi, M., Takamatsu, K., Saitoh, S., Miura, M., and Nogushi, T. (1992) *Biochem. Biophys. Res. Commun. 189*, 511−517.
19. Olafsson, P., Wang, T., and Lu, B. (1995) *Proc. Natl. Acad. Sci. U.S.A. 92*, 8001−8005.
20. Ames, J. B., Ishima, R., Tanaka, T., Gordon, J. I., Stryer, L., and Ikura, M (1997) *Nature 389*, 198−202.
21. Ames, J. B., Porumb, T., Tanaka, T., Ikura, M., and Stryer, L. (1995) *J. Biol. Chem. 270*, 4526−4533.
22. Monod, J., Wyman, J., and Changeux, J.-P. (1965) *J. Mol. Biol. 12*, 88−118.
23. Ray, S., Zozulya, S., Niemi, G. A., Flaherty, K. M., Brolley, D., Dizhoor, A. M., McKay, D. B., Hurley, J., and Stryer, L. (1992) *Proc. Natl. Acad. Sci. U.S.A. 89*, 5705−5709.
24. Ho, S. N., Hunt, H. D., Horton, R. M., Pullen, J. K., and Peas, L. R. (1989) *Gene (Amsterdam) 77*, 51−59.
25. Duronio, R. J., Jackson-Machelski, E., Heuckeroth, R., Olins, P. O., Devine, C. S., Yonemoto, W., Slice, L. W., Taylor, S. S., and Gordon, J. I. (1990) *Proc. Natl. Acad. Sci. U.S.A. 87*, 1506−1510.
26. Pace, C. N., Vajdos, F., Fee, L., Grimsley, G., and Gray, T. (1995) *Protein Sci. 4*, 2411−2423.
27. Tsien, R. Y. (1989) *Annu. Rev. Neurosci. 12*, 227−253.
28. Ladant, D. (1995) *J. Biol. Chem. 270*, 1−7.
29. Fung, B. K.-K., and Stryer, L. (1980) *Proc. Natl. Acad. Sci. U.S.A. 77*, 2500−2504.
30. Tsien, R., and Pozzan, T. (1989) *Methods Enzymol. 172*, 230−262.
31. Pethig, R., Kuhn, M., Payne, R., Adler, E., Chen, T.-H., and Jaffe, L. F. (1989) *Cell Calcium 10*, 491−498.
32. Bodenhausen, G., and Rubin, D. J. (1980) *Chem. Phys. Lett. 69*, 185−189.
33. Bax, A., Clore, G. M., and Gronenborn, A. M. (1990) *J. Magn. Reson. 88*, 425−431.
34. Kay, L. E., Keifer, P., and Saarinen, T. (1992) *J. Am. Chem. Soc. 114*, 10663−10665.
35. Zozulya, S., Ladant, D., and Stryer, L. (1995) *Methods Enzymol. 250*, 383−393.
36. Ames, J. B., Tanaka, T., Stryer L., and Ikura, M., (1996) *Curr. Opin. Struct. Biol. 6*, 432−438.
37. Eriksson, A. E., Baase, W. A., Zhang, X.-J., Heinz, D. W., Blaber, M., Baldwin, E. P., and Matthews, B. W. (1992) *Science 255*, 179−183.
38. Kirschner, M. W., and Schachman, H. K. (1973) *Biochemistry 12*, 2997−3004.
39. Schachman, H. K. (1988) *J. Biol. Chem. 263*, 18583−18586.
40. Fujimori, K., Sorenson, M., Herzberg, O., Moult, J., and Reinach, F. C. (1990) *Nature 345*, 182−184.
41. Pearlstone, J. R., Borgford, T., Chandra, M., Oikawa, K., Kay, C. M., Herzberg, O., Moult, J., Herklotz, A. Reinach, F. C., and Smillie, L. B. (1992) *Biochemistry 31*, 6545−6553.
42. Silva, C. R. da, Auaujo, A. H. B., Herzberg, O., Moult, J., Sorenson, M., and Reinach, F. C. (1993) *Eur. J. Biochem. 213*, 599−604.
43. Groves, P., Linse, S., Thurin, E., and Forsen, S. (1997) *Protein Sci. 6*, 323−330.
44. Nakayama, S., and Kretsinger, R. H. (1994) *Annu. Rev. Biomol. Struct. 23*, 473−507.
45. Palczewski, K., Subbaraya, I., Gorczyca, W. A., Helekar, B. S., Ruiz, C. C., Ohguro, H., Huang, J., Zhao, X., Crabb, J. W., Johnson, R. S., Walsh, K. A., Gray-Keller, M. P., Detwiler, P. B., and Baehr, W. (1994) *Neuron 13*, 395−404.
46. Dizhoor, A. M., Olshevskaya, E. V., Henzel, W. J., Wong, S. C., Stults, J. T., Ankoudinova, I., and Hurley, J. B. (1995) *J. Biol. Chem. 270*, 25200−25206.
47. Olshevskaya, E. V., Hughes, R. E., Hurley, J. B., and Dizhoor, A. M. (1997) *J. Biol. Chem. 272*, 14327−14333.

BI980928S